

# Crown ether conformations in 1,3-calix[4]arene bis(crown ethers): crystal structures of a caesium complex and solvent adducts and molecular dynamics simulations \*

Pierre Thuéry,<sup>a</sup> Martine Nierlich,<sup>a</sup> Jeffrey C. Bryan,<sup>b</sup> Véronique Lamare,<sup>c</sup> Jean-François Dozol,<sup>c</sup> Zouhair Asfari<sup>d</sup> and Jacques Vicens<sup>d</sup>

<sup>a</sup> CEASaclay, SCM (CNRS URA 331), Bât. 125, 91191 Gif-sur-Yvette, France

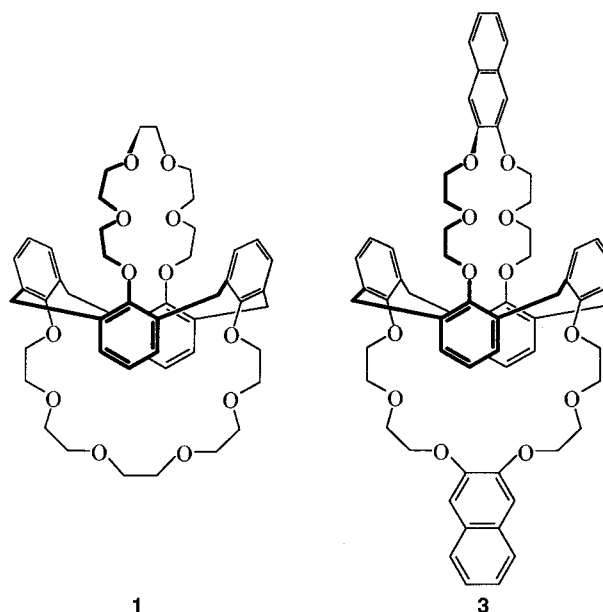
<sup>b</sup> Chemical Separations Group, Oak Ridge National Laboratory, Oak Ridge, TN 37831-6119, USA

<sup>c</sup> CEACadarache, SEPILPTE, 13108 Saint-Paul-lez-Durance, France

<sup>d</sup> ECPM, Laboratoire de Chimie des Interactions Moléculaires Spécifiques (CNRS URA 405), 1 rue Blaise Pascal, 67008 Strasbourg, France

The crystal structures of solvent adducts of 1,3-calix[4]arene bis(18-crown-6) **1** and 1,3-calix[4]arene bis(naphtho-18-crown-6) **3** as well as the structure of the caesium complex of **3** have been determined. In **1**·3CH<sub>3</sub>NO<sub>2</sub> and **3**·3CH<sub>3</sub>CN the complexed solvent molecules have their methyl group at the centre of the crown ether rings, whereas in **3**·C<sub>6</sub>H<sub>5</sub>CH<sub>3</sub>, the solvent is located in the crystal voids. The consequences on the crown ether conformations are noticeable: comparison with previous results shows that the conformation of **1** is only slightly different in its acetonitrile and nitromethane adducts, the conformation with acetonitrile being the same as in the caesium and potassium complexes; the conformation of the acetonitrile adduct of **3** is the same as that in the caesium complex and is strongly different from the one obtained by crystallization in toluene. Molecular dynamics simulations *in vacuo* were performed on free **3** and on its mononuclear caesium complex, and discussed in terms of the conformational mobility of the crown ether loop.

Among the various properties of calixarenes their ionophoric nature plays a prominent role and opens the way to some practical applications. In particular, the 1,3-calix[4]arene bis(crown ethers), in which the calixarene is locked in the 1,3-alternate conformation by crown ether bridging, constitute a family of ditopic receptors, some members of which have been shown to be suitable for the selective removal of caesium ions in nuclear wastes highly concentrated in sodium ions and strongly acidic.<sup>1-3</sup> Recently, these properties were shown to be retained in a basic medium.<sup>4</sup> In order better to understand the origins of this high selectivity, we are engaged in an investigation of the structural features of these compounds and their alkali-metal ion complexes, by single-crystal X-ray diffraction.<sup>5-9</sup> Some molecular dynamics simulations have also been performed with the aim of predicting the behaviour of new ligands.<sup>6,9,10</sup> In these simulations the structural complementarity between the cation and the ligand appears to be a primary criterion. From an energetic point of view, selectivity is due to the intrinsic ligand/cation affinity (always in favour of Na<sup>+</sup>) balanced by the desolvation energy of the cations (in favour of Cs<sup>+</sup>) as evidenced by molecular dynamics (MD)/free energy perturbation (FEP) calculations.<sup>10-12</sup> We have limited our structural investigations up to now to two ligands of this family: 1,3-calix[4]arene bis(18-crown-6) (**1**, see Scheme 1) and 1,3-calix[4]arene bis(benzo-18-crown-6) **2** which have been shown, from solution experiments, to present a high caesium over sodium selectivity. We have reported previously the crystal structures of acetonitrile adducts of **1**,<sup>6,8</sup> of its mono- and/or bi-nuclear caesium complexes with nitrate,<sup>6</sup> thiocyanate<sup>5</sup> or iodide<sup>7</sup> as counter ions and of its sodium and potassium complexes with nitrate counter ions.<sup>9</sup> We have also determined the crystal structures of the acetonitrile adduct of **2**,<sup>8</sup> and of its binuclear caesium complex with nitrate counter ions.<sup>5</sup> These structures indicate that the selectivity for caesium over sodium ions could be due to the



**Scheme 1** 1,3-Calix[4]arene bis(18-crown-6) **1** and 1,3-calix[4]arene bis(naphtho-18-crown-6) **3**. 18-crown-6 = 1,4,7,10,13,16-Hexaoxacyclooctadecane; naphtho-18-crown-6 = 7,8,11,13,14,16,17,19,20-decahydronaphtho[2,3-*b*][1,4,7,10,13,16]hexaoxacyclooctadecane

cation/ligand structural complementarity and the preorganization of **1**, or **2**, for the complexation of CsNO<sub>3</sub>. The less favoured sodium complexation by **1** involves only three crown ether oxygen atoms and necessitates a ligand reorganization. Some new structures are described in the present paper: the first is that of **1** with nitromethane, a solvent similar to acetonitrile in size and polarity; the three others are those of **3** (see Scheme 1) with acetonitrile and with toluene, and of its binuclear caesium complex.

\* Non-SI unit employed: D ≈ 3.33 × 10<sup>-30</sup> C m.

## Experimental

### Synthesis

**1,3-Calix[4]arene bis(18-crown-6)·3CH<sub>3</sub>NO<sub>2</sub>·1·3CH<sub>3</sub>NO<sub>2</sub>.** Compound **1** was prepared as described elsewhere<sup>1</sup> (Found: C, 70.23; H, 6.92. Calc.: C, 70.02; H, 7.18%). Its recrystallization from nitromethane yielded colourless single crystals of 1·3CH<sub>3</sub>NO<sub>2</sub> suitable for X-ray crystallography.

**1,3-Calix[4]arene bis(naphtho-18-crown-6)·3CH<sub>3</sub>CN·3·3CH<sub>3</sub>CN and 1,3-calix[4]arene bis(naphtho-18-crown-6)·C<sub>6</sub>H<sub>5</sub>CH<sub>3</sub>·3·C<sub>6</sub>H<sub>5</sub>CH<sub>3</sub>.** Compound **3** was prepared as described elsewhere<sup>1</sup> (Found: C, 74.90; H, 6.35. Calc.: C, 74.97; H, 6.30%). Its recrystallization from acetonitrile or hot toluene yielded colourless single crystals of 3·3CH<sub>3</sub>CN or 3·C<sub>6</sub>H<sub>5</sub>CH<sub>3</sub>, respectively, suitable for X-ray crystallography.

**2Cs<sup>+</sup>·2NO<sub>3</sub><sup>-</sup>·3·CHCl<sub>3</sub>·C<sub>4</sub>H<sub>8</sub>O·H<sub>2</sub>O** **4**. Compound **3** (0.2 mmol), dissolved in acetonitrile–chloroform (1:1, 10 cm<sup>3</sup>) was treated with a large excess of CsNO<sub>3</sub> (2.5 mmol), at room temperature, during 8 h. Unchanged CsNO<sub>3</sub> was then filtered off. The resulting powder was recrystallized several times, and finally from tetrahydrofuran–chloroform (1:1), yielding beautiful colourless crystals of **4** suitable for X-ray crystallography.

### <sup>1</sup>H and <sup>133</sup>Cs NMR spectroscopy

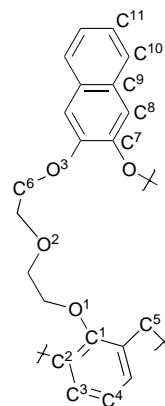
Proton NMR spectra were measured on Bruker SY200 and AM400 instruments, <sup>133</sup>Cs NMR at 52.5 MHz in the pulse Fourier-transform mode on a Bruker AM400 spectrometer. A 0.5 M aqueous CsBr solution was used as an external reference. The <sup>133</sup>Cs chemical shifts of Cs<sup>+</sup>SCN<sup>-</sup> [0.05 M in CD<sub>3</sub>OD–CDCl<sub>3</sub> (2:3)] was monitored in the presence of different amounts of ligands. Solubilization of the samples was performed through ultrasonication and spectra were measured at regular intervals after 6 h, until equilibrium appeared to be reached.

### Electron spray mass spectrometry (ESMS)

The ESMS studies were performed on a VG Bio Q triple quadrupole mass spectrometer upgraded in order to obtain the Quattro II performances (Micromass, Altrincham, UK).

### Crystallography

The crystals were sealed in thin-walled capillaries (1·3CH<sub>3</sub>NO<sub>2</sub>, 3·3CH<sub>3</sub>CN and **4**) or mounted on a glass fibre (3·C<sub>6</sub>H<sub>5</sub>CH<sub>3</sub>). The diffraction experiments were performed with an Enraf-Nonius CAD4 diffractometer using Mo–Kα (λ 0.710 73 Å) radiation. Crystal data are given in Table 1, together with refinement details. The lattice parameters were determined from the least-squares refinement of the setting angles of 25 reflections (8 < θ < 12°). The data were collected in the range 1 < θ < 20° for compounds 1·3CH<sub>3</sub>NO<sub>2</sub>, 3·3CH<sub>3</sub>CN and **4**, since very few reflections were measured above 20°, due to the rather low crystal quality, and in the range 1 < θ < 23° for 3·C<sub>6</sub>H<sub>5</sub>CH<sub>3</sub>. The intensity decay was estimated from three standard reflections and linearly corrected. The data were corrected for Lorentz-polarization effects. No absorption corrections were made. Structures of compounds **1** and **3** were solved by direct methods with SHELXS 86<sup>13</sup> and that of **4** by the heavy-atom method; subsequent Fourier syntheses were used to determine remaining non-hydrogen atomic positions. The refinement was done by full-matrix least squares on *F* for compounds 1·3CH<sub>3</sub>NO<sub>2</sub>, 3·3CH<sub>3</sub>CN and **4** and on *F*<sup>2</sup> for 3·C<sub>6</sub>H<sub>5</sub>CH<sub>3</sub>. Analytical scattering factors for neutral atoms<sup>14</sup> were corrected for the anomalous dispersion terms Δ*f*' and Δ*f*". The enantiomorph was checked to give the same *R* factor for compound **4**. Hydrogen atoms were located at their ideal positions (C–H 0.95 Å; *B* = 6 Å<sup>2</sup> for 1·3CH<sub>3</sub>NO<sub>2</sub>, 3·3CH<sub>3</sub>CN and **4**, *B* = 1.2 (CH, CH<sub>2</sub>) or 1.5 (CH<sub>3</sub>) times the equivalent isotropic displacement parameter of the attached carbon atom for 3·C<sub>6</sub>H<sub>5</sub>CH<sub>3</sub>) and constrained to



C <sup>1</sup> : 0.185	O <sup>1</sup> , O <sup>3</sup> : -0.35
C <sup>2</sup> : -0.204	O <sup>2</sup> : -0.42
C <sup>3</sup> : -0.037	H <sup>3</sup> : 0.077
C <sup>4</sup> : -0.075	H <sup>4</sup> : 0.078
C <sup>5</sup> : 0.190	H <sup>5</sup> : 0.045
C <sup>6</sup> : 0.213	H <sup>6</sup> : 0.000
C <sup>7</sup> : 0.088	H <sup>8</sup> , H <sup>10</sup> : 0.089
C <sup>8</sup> : -0.046	H <sup>11</sup> : 0.075
C <sup>9</sup> : -0.050	
C <sup>10</sup> : -0.046	
C <sup>11</sup> : -0.071	

**Scheme 2** Point charges calculated on compound **3** (from MNDO scaled charges calculated on half a calixcrown)

ride on their parent carbon atom. All calculations have been performed on a Vax 4000-200 computer with the Enraf-Nonius MOLEN system<sup>15</sup> for 1·3CH<sub>3</sub>NO<sub>2</sub>, 3·3CH<sub>3</sub>CN and **4** and on a Silicon Graphics Indigo 2XZ computer with XCAD 4<sup>16</sup> (data reduction), SHELXTL<sup>17</sup> (structure solution and refinement) and PLATON<sup>18</sup> (geometry analysis) for 3·C<sub>6</sub>H<sub>5</sub>CH<sub>3</sub>. The molecular drawings were done with ORTEP II.<sup>19</sup> Special features concerning disorder, anisotropic parameters and some refinement details are described below.

**1·3CH<sub>3</sub>NO<sub>2</sub>.** Anisotropic parameters were refined for oxygen atoms of the crowns and oxygen, nitrogen and carbon atoms of the solvent molecules.

**3·3CH<sub>3</sub>CN.** The acetonitrile molecule not included in the crown ether chains was highly disordered and was fixed in the last refinement cycles. Anisotropic parameters were refined for oxygen atoms and for the nitrogen and carbon atoms of the included acetonitrile molecules.

**3·C<sub>6</sub>H<sub>5</sub>CH<sub>3</sub>.** Two positions were found for the toluene molecule which were refined with occupancies of 0.8 and 0.2. The C–CH<sub>3</sub> distances on each were restrained to be 1.52 Å. The weighting scheme used was  $w = 1/[\sigma^2(F_o^2) + (0.0627P)^2 + 0.7553P]$ , where  $P = (F_o^2 + 2F_c^2)/3$ .

**4.** Anisotropic parameters were refined for caesium, chlorine and oxygen atoms (except the oxygen atom of the water molecule and that of the tetrahydrofuran molecule, which was not identified).

CCDC reference number 186/705.

### Computational methods

All calculations were carried out on a SG INDIGO 2 R8000 workstation with the AMBER 4.1 software,<sup>20</sup> using, as a force field, the all-atom parameters and the potential energy as expressed in equation (1) where *r*, θ and φ represent the bond

$$E_{\text{pot}} = \sum_{\text{bonds}} K_r(r - r_{\text{eq}})^2 + \sum_{\text{angles}} K_\theta(\theta - \theta_{\text{eq}})^2 + \sum_{\text{dihedrals}} \frac{V_n}{2} [1 + \cos(n\phi - \eta)] + \sum_{i < j} \left\{ \epsilon_{ij} \left[ \left( \frac{R^*}{R_{ij}} \right)^{12} - \left( \frac{R^*}{R_{ij}} \right)^6 \right] \right\} + \sum_{i < j} \left( \frac{q_i q_j}{\epsilon R_{ij}} \right) + \sum_{\text{H bonds}} \left\{ \epsilon_{ij} \left[ \left( \frac{R^*}{R_{ij}} \right)^{12} - \left( \frac{R^*}{R_{ij}} \right)^{10} \right] \right\} \quad (1)$$

length, bond angle and dihedral angle respectively, *R<sub>ij</sub>* the distance between atoms *i* and *j*, *q<sub>i</sub>* and *q<sub>j</sub>* the atomic charges on atoms *i* and *j*, and ε the relative permittivity.<sup>21</sup> The calixcrown **3** was model-built with the SYBYL software<sup>22</sup> from the previously studied derivative **2**<sup>10</sup> and submitted to a first minimiz-

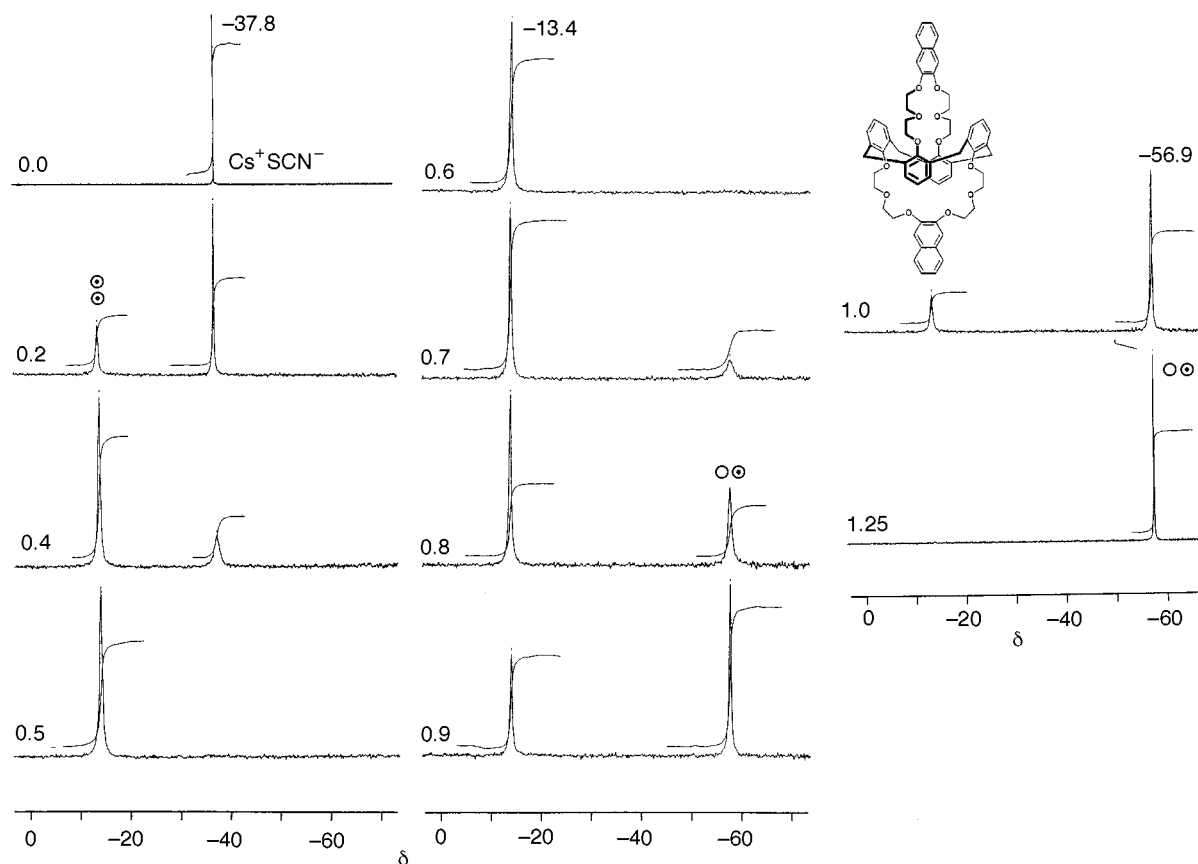


Fig. 1 The  $^{133}\text{Cs}$  NMR spectra of  $\text{Cs}^+\text{SCN}^-$  with **3** in  $\text{CD}_3\text{OD}-\text{CDCl}_3$  (2:3). The calixarene:  $\text{Cs}^+$  ratios are indicated

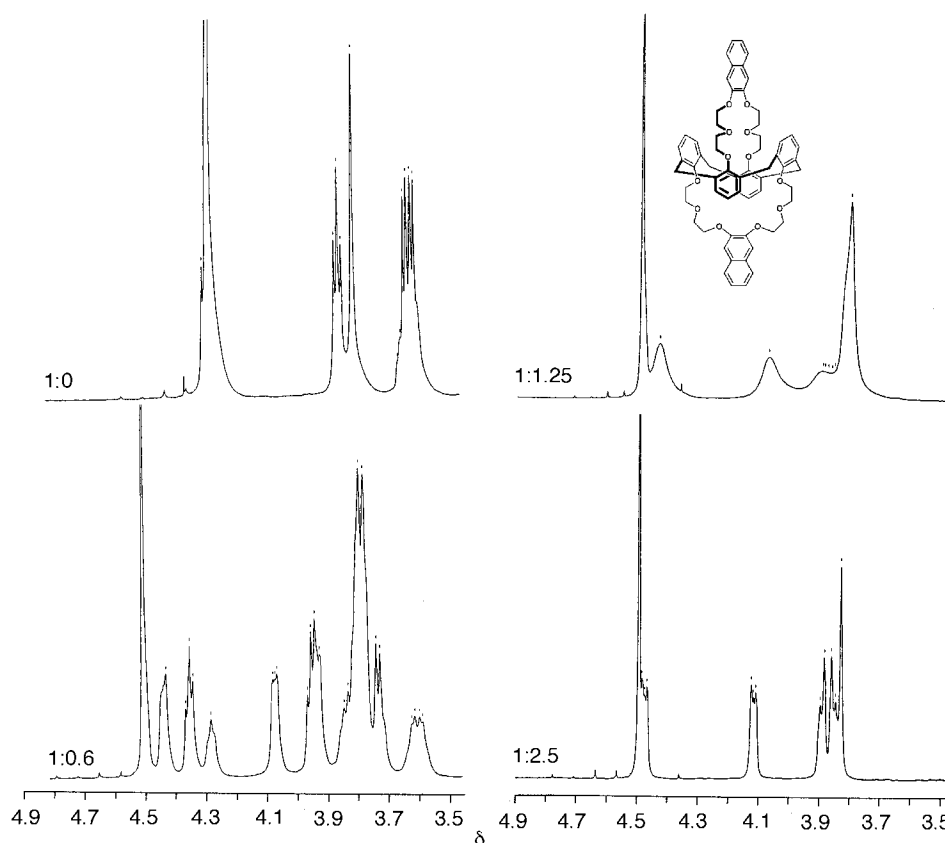
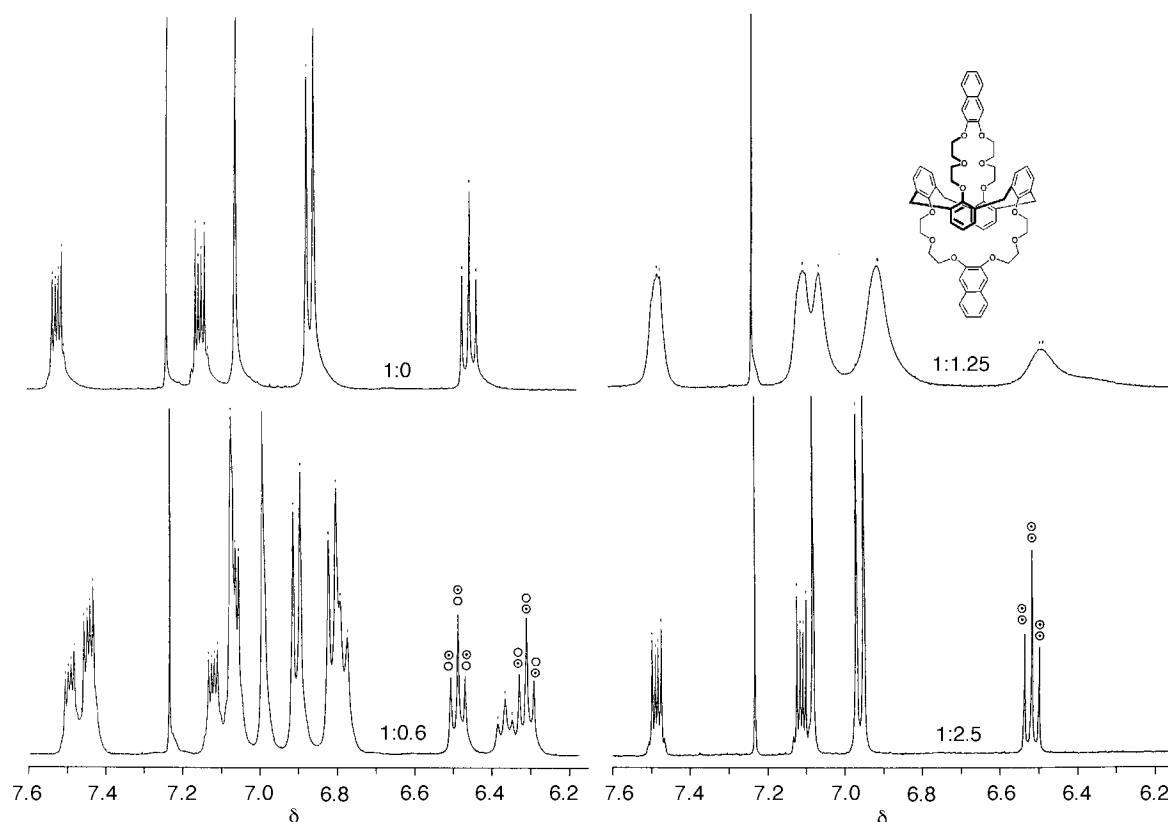


Fig. 2 Proton NMR spectra (400 MHz, 25 °C) of the glycolic region of compound **3** with 0.05 M  $\text{Cs}^+\text{SCN}^-$  in  $\text{CD}_3\text{OD}-\text{CDCl}_3$  (2:3). The calixarene:  $\text{Cs}^+$  ratios are indicated

ation. The atomic charges on the calixarene were calculated on half the calixcrown with the minimum neglect of differential overlap (MNDO) semiempirical method, then averaged for

equivalent atoms and scaled up with a 1.26 scaling factor to allow a nice fit with the 6-31G\*/ESP values commonly used for crown ether moieties.<sup>23</sup> It is noticeable that, with this protocol,



**Fig. 3** Proton NMR spectra (400 MHz, 25 °C) of the aromatic region of compound **3** with 0.05 M Cs<sup>+</sup>SCN<sup>-</sup> in CD<sub>3</sub>OD–CDCl<sub>3</sub> (2:3). The calixarene:Cs<sup>+</sup> ratios are indicated

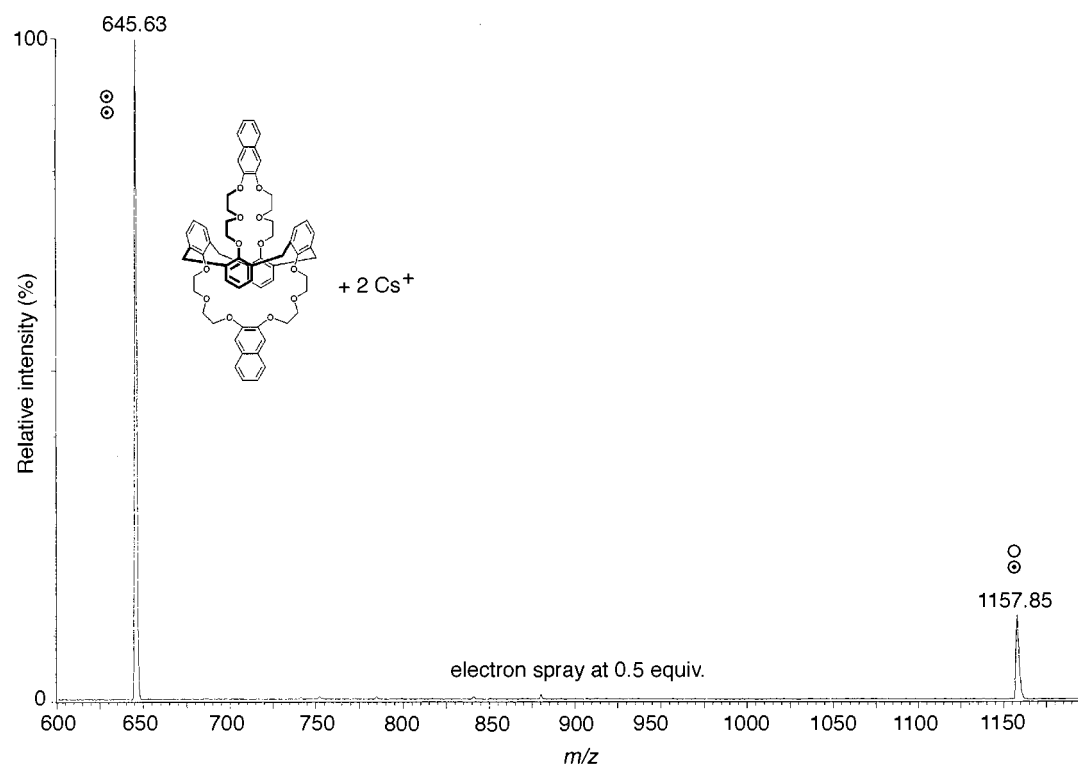


**Fig. 4** Electron spray mass spectrum of a CD<sub>3</sub>OD–CDCl<sub>3</sub> (2:3) solution of compound **3** and Cs<sup>+</sup>SCN<sup>-</sup> (1:0.5)

the partial charges calculated on the oxygen atoms are greatly influenced by the proximity of unsaturated rings and range from  $-0.35$  to  $-0.42$  (see Scheme 2). The ion parameters came from Åqvist<sup>24</sup> and were adapted to the AMBER force field (TIP3P water model and periodic boundary conditions). Parameters for the nitrate anion were taken from Guilbaud and

Wipff.<sup>25</sup> The 1–4 non-bonded contributions were scaled down by a factor of 0.5.

The structures of **3**, **3**·Cs<sup>+</sup> and **3**·CsNO<sub>3</sub> were first submitted to 2000 steps of minimization then to at least 1 ns of molecular dynamics *in vacuo* at 300 K with a time step of 1.0 fs, a 10 Å residue-based cut-off and a relative permittivity set to 1.0.

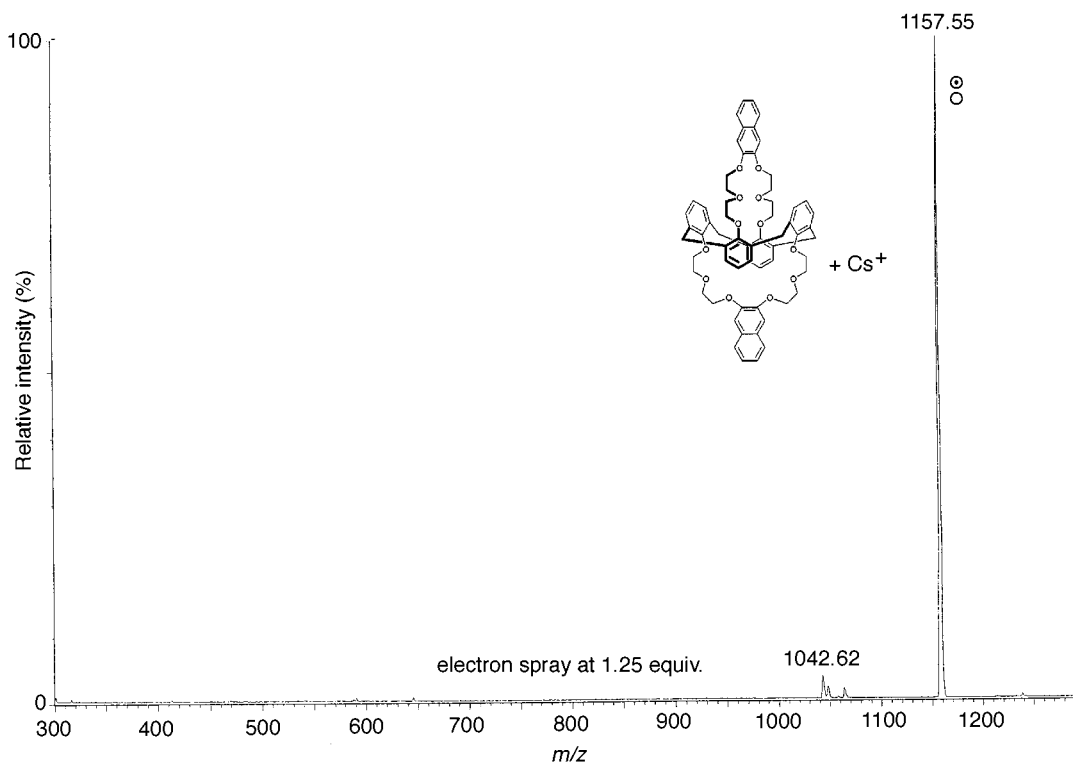


Fig. 5 Electron spray mass spectrum of a  $\text{CD}_3\text{OD}-\text{CDCl}_3$  (2:3) solution of compound **3** and  $\text{Cs}^+\text{SCN}^-$  (1:1.25)

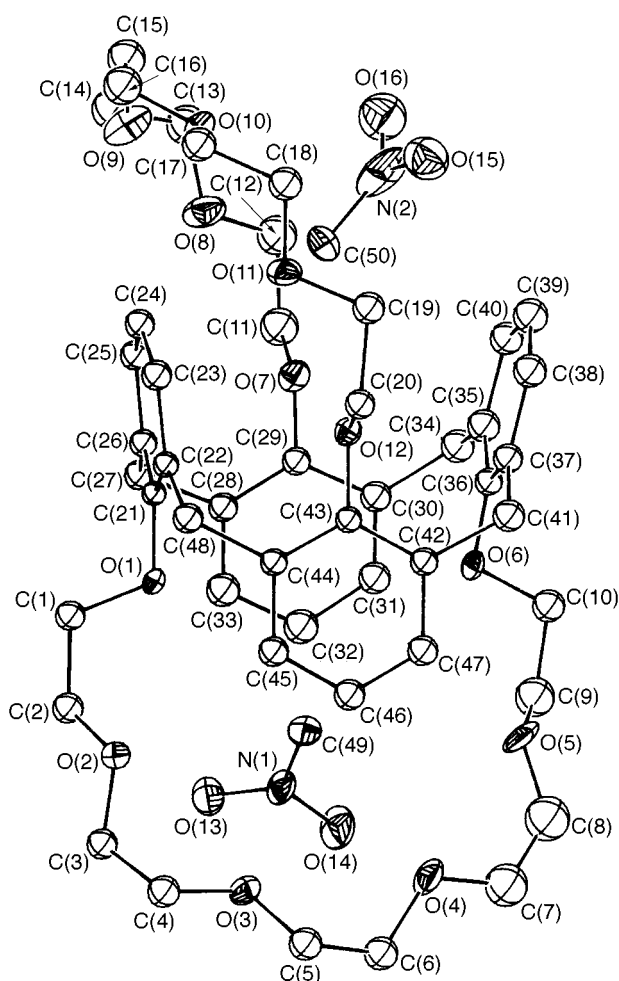


Fig. 6 Molecular unit of  $1 \cdot 3\text{CH}_3\text{NO}_2$ . Uncomplexed solvent molecule omitted

One conformation was saved every ps and the subsequent trajectories were visualized by the MD/DRAW software and ana-

lysed by the MDS software.<sup>26</sup> The first five ps, corresponding to the equilibration of the systems, were not taken into account in the analysis and averages were calculated over 995 ps of MD run.

## Results and Discussion

### NMR and ESMS

Ikeda *et al.*<sup>27</sup> and Beer *et al.*<sup>28</sup> were the first to report that the 1,3-alternate conformer of O-substituted derivatives of *p*-tert-butylcalix[4]arene can form both mono- and bi-nuclear complexes with alkali-metal cations. The O-tetraester<sup>27</sup> was shown to form 1:1 and 2:1 metal-ligand complexes with sodium ions while the O-tetramide<sup>28</sup> formed similar complexes with potassium. In our previous papers,<sup>5-9</sup> we have reported a series of 1:1 and 2:1 alkali metal-1,3-calix[4]arene bis(crown ether) complexes which were structurally characterized.

The co-ordination mode of caesium ions by compound **3** has been investigated by means of  $^1\text{H}$  and  $^{133}\text{Cs}$  NMR techniques and electron spray mass spectroscopy. The co-ordination is clearly evidenced on Fig. 1: the  $^{133}\text{Cs}$  chemical shift at  $\delta -37.8$  of free  $\text{Cs}^+\text{SCN}^-$  in  $\text{CD}_3\text{OD}-\text{CDCl}_3$  (2:3) solution is shifted to  $\delta -56.9$  for the mononuclear species  $3 \cdot \text{Cs}^+$ , while a signal at  $\delta -13.4$  is observed for the corresponding binuclear species  $3 \cdot 2\text{Cs}^+$ . These values match the ones obtained for **1** and related complexes.<sup>29</sup> Further information is obtained by comparing the  $^1\text{H}$  NMR spectrum of **3** with those of the  $3 \cdot \text{Cs}^+$  and  $3 \cdot 2\text{Cs}^+$  complexes. The 400 MHz  $^1\text{H}$  NMR spectra were obtained with the same  $\text{CD}_3\text{OD}-\text{CDCl}_3$  (2:3) titration solutions as for the  $^{133}\text{Cs}$  NMR spectra. As illustrated on Fig. 2 the signals of the polyether protons of free **3** are split into several signals upon addition of  $\text{Cs}^+\text{SCN}^-$ . A coalescence is observed for a **3**: $\text{Cs}^+$  ratio = 1:1.25. Then further addition of caesium salt up to a **3**: $\text{Cs}^+$  ratio = 1:2.5 leads to a more symmetric spectrum. The first conclusion which can be drawn from these observations is that the caesium complexation occurs in the polyether loops of **3**. Further information is provided by  $^1\text{H}$  NMR chemical shift changes in the aromatic region of the spectrum of **3** (Fig. 3). One can see that the triplet at  $\delta 6.41$  of free **3** (*p*-H of aryl) is split into two distinct triplets at  $\delta 6.52$  and  $6.35$  corresponding

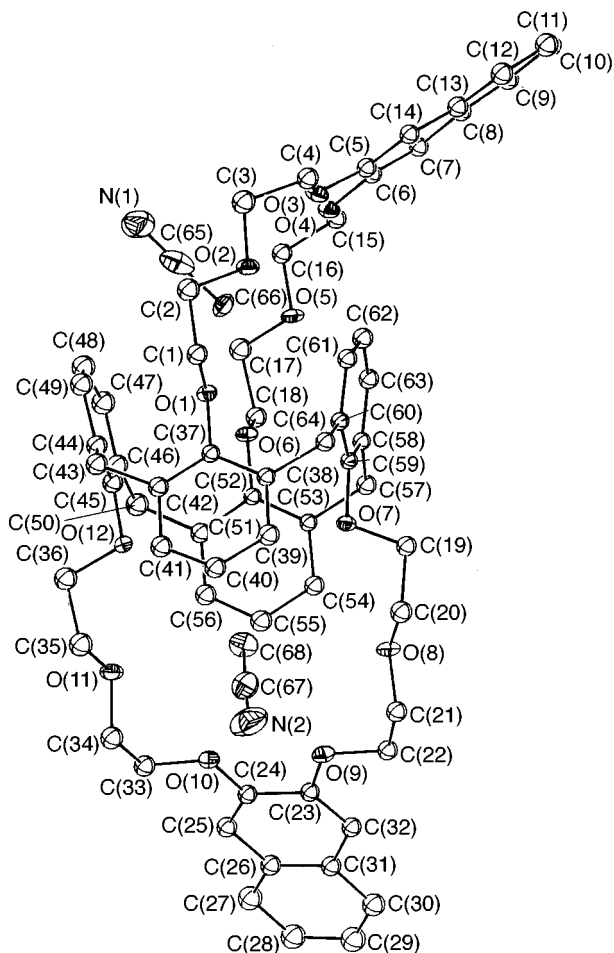


Fig. 7 Molecular unit of  $3 \cdot 3\text{CH}_3\text{CN}$ . Uncomplexed solvent molecule omitted

to empty and filled cavities of the unsymmetrical mononuclear species  $3 \cdot \text{Cs}^+$  (as seen for a  $3 : \text{Cs}^+$  ratio = 1:0.6). When  $3 : \text{Cs}^+ = 1:1.25$  we observe coalescence as in the glycolic region of the spectrum. This can be attributed to a rapid metal–ligand exchange between mono- and bi-nuclear species. When the ratio  $3 : \text{Cs}^+$  is equal to 1:2.5 a well resolved triplet only is detected at  $\delta$  6.55, associated with the symmetric binuclear species. Similar results have been obtained in the case of **1**,<sup>6</sup> and interpreted in terms of formation of asymmetric mononuclear species when the calixarene: $\text{Cs}^+$  ratio is greater than unity (with slow interchange of the cation between the two crown ether loops), a rapid cation–ligand exchange between mono- and bi-nuclear species when the ratio is near unity and formation of binuclear species when the ratio is lower than unity. These observations are confirmed by mass spectroscopy measurements: FAB (positive) mass spectrometry performed directly on the  $\text{CD}_3\text{OD}-\text{CDCl}_3$  (2:3) titration solutions allowed the detection of  $3 \cdot \text{Cs}^+$  only, whereas electron spray mass spectroscopy permitted the detection of  $3 \cdot \text{Cs}^+$ ,  $[\text{M} + \text{Cs}]^+$ , at  $m/z$  1157.55 and  $3 \cdot 2\text{Cs}^+$  at  $m/z$  645.63 as depicted in Figs. 4 and 5.

### Crystal structures

Drawings of the compounds under study, including the atom numbering scheme, are presented in Figs. 6–10, selected bond lengths and angles are given in Table 2 and selected torsion angles in Table 3.

In  $1 \cdot 3\text{CH}_3\text{NO}_2$  the conformations of the two crowns can be described as suggested by Fyles and Gandour<sup>30</sup> by the sequence of O–C–O torsion *gauche* angles  $g^+g^-g^+(\approx 16^\circ)g^-$  and  $g^-g^+g^-g^+$ , with some deviations of the *anti* C–O–C angles from the ideal value. They are different from the conformations

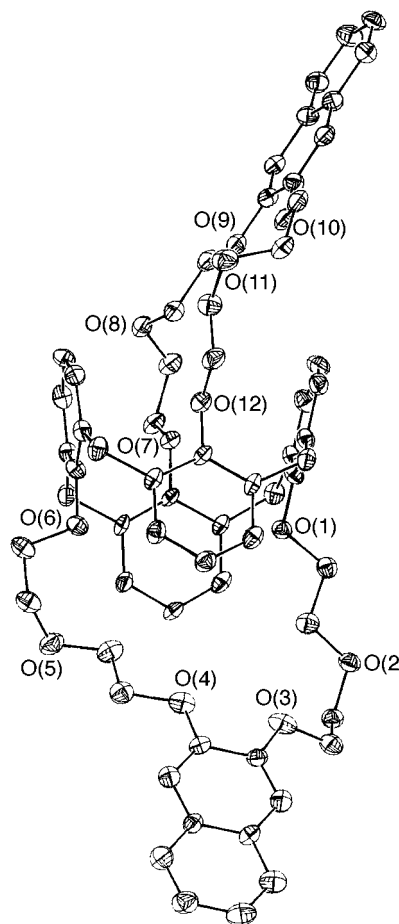


Fig. 8 Molecular unit of  $3 \cdot \text{C}_6\text{H}_5\text{CH}_3$ . Solvent molecule omitted. Atom numbering scheme identical to that in Fig. 7

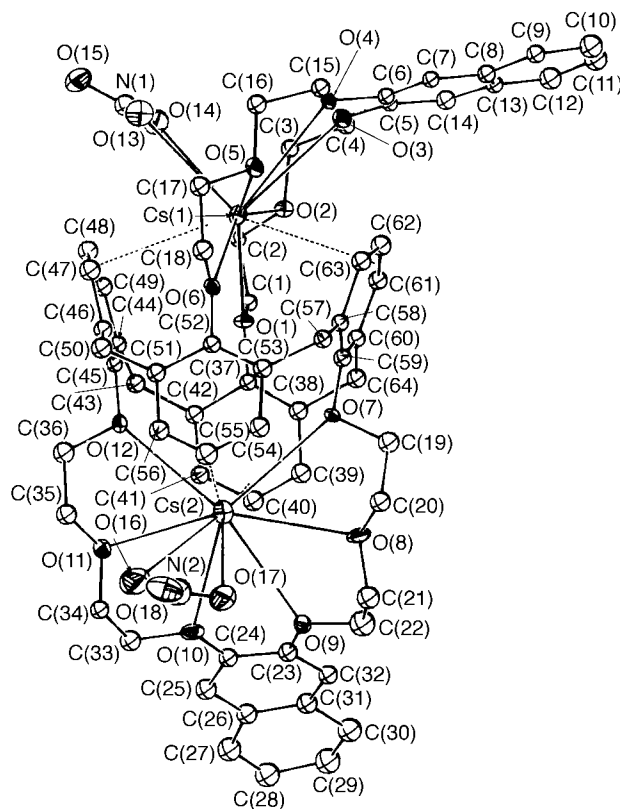


Fig. 9 Molecular unit of  $2\text{Cs}^+ \cdot 2\text{NO}_3^- \cdot 3 \cdot \text{CHCl}_3 \cdot \text{C}_4\text{H}_8\text{O} \cdot \text{H}_2\text{O}$  **4**. Solvent molecules omitted

in the acetonitrile adducts  $1 \cdot 4\text{CH}_3\text{CN}$ <sup>6</sup> and  $1 \cdot 3\text{CH}_3\text{CN}$ <sup>8</sup> which are  $g^+g^-g^+g^-g^+$  or  $g^+g^-0g^+g^-$ . This difference does not repre-

**Table 1** Crystal data and structure refinement details

	<b>1</b> ·3CH <sub>3</sub> NO <sub>2</sub>	<b>3</b> ·3CH <sub>3</sub> CN	<b>3</b> ·C <sub>6</sub> H <sub>5</sub> CH <sub>3</sub>	<b>4</b>
Empirical formula	C <sub>51</sub> H <sub>69</sub> N <sub>3</sub> O <sub>18</sub>	C <sub>70</sub> H <sub>73</sub> N <sub>3</sub> O <sub>12</sub>	C <sub>71</sub> H <sub>72</sub> O <sub>12</sub>	C <sub>69</sub> H <sub>75</sub> Cl <sub>3</sub> C <sub>52</sub> N <sub>2</sub> O <sub>20</sub>
<i>M</i>	1012.13	1148.38	1117.3	1624.54
Crystal system	Triclinic	Monoclinic	Monoclinic	Monoclinic
Space group	<i>P</i> $\bar{1}$	<i>P2</i> <sub>1</sub> / <i>c</i>	<i>P2</i> <sub>1</sub> / <i>n</i>	<i>Pn</i>
<i>a</i> /Å	11.085(3)	13.876(5)	20.815(2)	14.602(2)
<i>b</i> /Å	11.758(4)	21.834(9)	10.697(1)	18.226(6)
<i>c</i> /Å	21.203(9)	21.472(4)	26.222(3)	15.442(4)
$\alpha$ /°	83.22(3)			
$\beta$ /°	75.50(3)	104.49(2)	90.696(8)	113.89(2)
$\gamma$ /°	83.10(2)			
<i>U</i> /Å <sup>3</sup>	2645(3)	6298(7)	5838(1)	3758(3)
<i>Z</i>	2	4	4	2
<i>D<sub>c</sub></i> /Mg m <sup>-3</sup>	1.271	1.211	1.27	1.436
$\mu$ /mm <sup>-1</sup>	0.090	0.077	0.09	1.135
Crystal size/mm	0.6 × 0.5 × 0.4	0.6 × 0.5 × 0.5	0.5 × 0.4 × 0.2	0.6 × 0.5 × 0.4
$\theta$ Range/°	1–20	1–20	2–23	1–20
<i>T</i> /K	295	295	163	295
<i>F</i> (000)	1080	2440	2376	1648
Scan type	$\omega$ – $\theta$	$\omega$ – $\theta$	$\omega$	$\omega$ – $\theta$
<i>hkl</i> Index ranges	[–10, 10] [0, 11] [–20, 20]	[–13, 13] [0, 21] [–20, 0]	[0, 22] [0, 11] [–28, 28]	[–14, 14] [0, 17] [0, 14]
Intensity decay (%)	18.8 in 50 h	3.1 in 34 h	7.0 in 93 h	1.6 in 49 h
Reflections collected	5265	6284	9532	3838
Independent reflections	4937	5858	8101	3507
<i>R</i> <sub>int</sub>	0.008	0.014	0.040	0.017
Observed reflections	2980 [ <i>I</i> > 3 $\sigma$ ( <i>I</i> )]	3024 [ <i>I</i> > 3 $\sigma$ ( <i>I</i> )]	5277 [ <i>F</i> <sup>2</sup> > 2 $\sigma$ ( <i>F</i> <sup>2</sup> )]	3333 [ <i>I</i> > 1 $\sigma$ ( <i>I</i> )]
Number of parameters	409	419	790	498
<i>R</i>	0.110	0.102	0.047	0.059
<i>R</i> '	0.105 ( <i>w</i> = 1)	0.105 ( <i>w</i> = 1)	0.129 (see text)	0.064 ( <i>w</i> = 1)
Largest residual electron density/e Å <sup>-3</sup>	0.77, –0.12	0.41, –0.11	0.31, –0.31	0.78, –0.13

**Table 2** Selected bond lengths (Å) and angles (°) in the environment of the caesium ion in compound **4**

Cs(1)–O(1)	3.22(1)	Cs(2)–O(7)	3.37(1)
Cs(1)–O(2)	3.08(1)	Cs(2)–O(8)	3.17(2)
Cs(1)–O(3)	3.51(1)	Cs(2)–O(9)	3.51(2)
Cs(1)–O(4)	3.57(1)	Cs(2)–O(10)	3.47(2)
Cs(1)–O(5)	3.16(1)	Cs(2)–O(11)	3.16(1)
Cs(1)–O(6)	3.22(1)	Cs(2)–O(12)	3.16(1)
Cs(1)–O(13)	3.31(2)	Cs(2)–O(16)	3.32(3)
Cs(1)–O(14)	3.18(2)	Cs(2)–O(17)	3.10(3)
Cs(1)···C(47)	3.70(2)	Cs(2)···C(39)	3.57(3)
Cs(1)···C(48)	3.52(2)	Cs(2)···C(40)	3.38(3)
Cs(1)···C(49)	3.76(2)	Cs(2)···C(41)	3.51(3)
Cs(1)···C(61)	3.57(3)	Cs(2)···C(54)	3.82(2)
Cs(1)···C(62)	3.41(2)	Cs(2)···C(55)	3.54(2)
Cs(1)···C(63)	3.56(2)	Cs(2)···C(56)	3.66(3)
O(1)–Cs(1)–O(2)	3.8(3)	O(7)–Cs(2)–O(8)	51.7(3)
O(1)–Cs(1)–O(13)	134.5(4)	O(7)–Cs(2)–O(16)	136.7(8)
O(1)–Cs(1)–O(14)	104.1(4)	O(7)–Cs(2)–O(17)	111.7(6)
O(2)–Cs(1)–O(3)	52.2(3)	O(8)–Cs(2)–O(9)	50.3(4)
O(2)–Cs(1)–O(13)	114.0(4)	O(8)–Cs(2)–O(16)	121.5(7)
O(2)–Cs(1)–O(14)	75.7(4)	O(8)–Cs(2)–O(17)	84.1(6)
O(3)–Cs(1)–O(4)	43.0(3)	O(9)–Cs(2)–O(10)	43.1(3)
O(3)–Cs(1)–O(13)	95.9(4)	O(9)–Cs(2)–O(16)	104.2(5)
O(3)–Cs(1)–O(14)	79.1(4)	O(9)–Cs(2)–O(17)	83.0(5)
O(4)–Cs(1)–O(5)	49.9(3)	O(10)–Cs(2)–O(11)	51.9(4)
O(4)–Cs(1)–O(13)	78.9(4)	O(10)–Cs(2)–O(16)	82.1(7)
O(4)–Cs(1)–O(14)	90.4(4)	O(10)–Cs(2)–O(17)	86.7(5)
O(5)–Cs(1)–O(6)	54.3(3)	O(11)–Cs(2)–O(12)	56.0(3)
O(5)–Cs(1)–O(13)	68.8(4)	O(11)–Cs(2)–O(16)	66.9(8)
O(5)–Cs(1)–O(14)	104.9(5)	O(11)–Cs(2)–O(17)	99.0(6)
O(6)–Cs(1)–O(1)	99.6(3)	O(12)–Cs(2)–O(7)	97.7(3)
O(6)–Cs(1)–O(13)	93.0(4)	O(12)–Cs(2)–O(16)	88.8(6)
O(6)–Cs(1)–O(14)	127.7(4)	O(12)–Cs(2)–O(17)	123.8(5)
O(13)–Cs(1)–O(14)	39.3(5)	O(16)–Cs(2)–O(17)	37.5(7)

sent an important reorganization of the crowns, but indicates that, even with solvents rather similar in size and in polarity (3.924 D for acetonitrile and 3.46 D for nitromethane<sup>31</sup>) and both possessing a methyl group suitable for inclusion in the crown, there is some solvent effect on the crown conformation.

These conformations enable all the oxygen lone pairs to be directed towards the central molecule or ion. The occurrence of the conformations encountered so far in **1** as well as in 1,3-calix[4]arene mono(18-crown-6) **5**,<sup>32</sup> **2** and **3** is given in Table 4:  $g^+g^-g^+g^-g^+$  is the most common conformation in **1** and is encountered both in acetonitrile- or CsNO<sub>3</sub>-complexing species. The location of the two complexed nitromethane molecules in **1**·3CH<sub>3</sub>NO<sub>2</sub> is very similar to the one of acetonitrile in **1**·4CH<sub>3</sub>CN and **1**·3CH<sub>3</sub>CN (molecular dynamics simulations in solution predict a location of acetonitrile in the adduct of **1** very close to what we observe in the solid state<sup>12</sup>). The methyl groups lie near the centre of the crowns [C···O distances between 3.21 and 3.77: mean 3.5(2) Å], *i.e.* very near to the position occupied by the caesium ions in the complexes, and the C–N bond is nearly perpendicular to the crown ether mean plane. The six oxygen atoms of each crown lie in a plane with a deviation of  $\pm 0.24(1)$  and  $\pm 0.42(1)$  Å respectively, the methyl groups being at 1.05(1) and 1.31(2) Å respectively from these mean planes. A third nitromethane molecule is present in the packing, without any particular interaction with **1**. This structure can be compared with those of crown ethers with nitromethane. In the case of 18-crown-6<sup>33</sup> the methyl–oxygen distances are in the range 3.25(2)–3.55(2) Å and the complexation has been attributed to weak CH···O hydrogen bonds. However, in our case, the opening of the ring due to the calixarene presence makes the diameter comparable to that of 21-crown-7 (1,4,7,10,13,16,19-heptaaxacyclohencosane) more than to that of 18-crown-6: in the nitromethane complex of dibenzo-21-crown-7 (6,7,9,10,12,13,20,21,23,24-decahydrodibenzo[*b,k*][1,4,7,10,13,16,19]-heptaaxacyclohencosine) the methyl–oxygen distances are in the range 3.272(3)–3.561(6) (mean 3.47) Å,<sup>34</sup> close to those in 18-crown-6 complexes and in **1**·3CH<sub>3</sub>NO<sub>2</sub>.

The effect of the solvent on the crown conformation is more clear cut with the **3** structures. The crown ether conformation is identical in the acetonitrile adduct **3**·3CH<sub>3</sub>CN and the caesium complex **4**, with the sequence  $g^+g^-0g^+g^-$ , the same as in the solvent adducts **2**·3CH<sub>3</sub>CN,<sup>8</sup> **2**·3CH<sub>3</sub>NO<sub>2</sub><sup>35</sup> and the caesium complex **2**Cs<sup>+</sup>·2NO<sub>3</sub><sup>-</sup>·**2**·3CHCl<sub>3</sub> (**6**).<sup>5</sup> This conformation, with

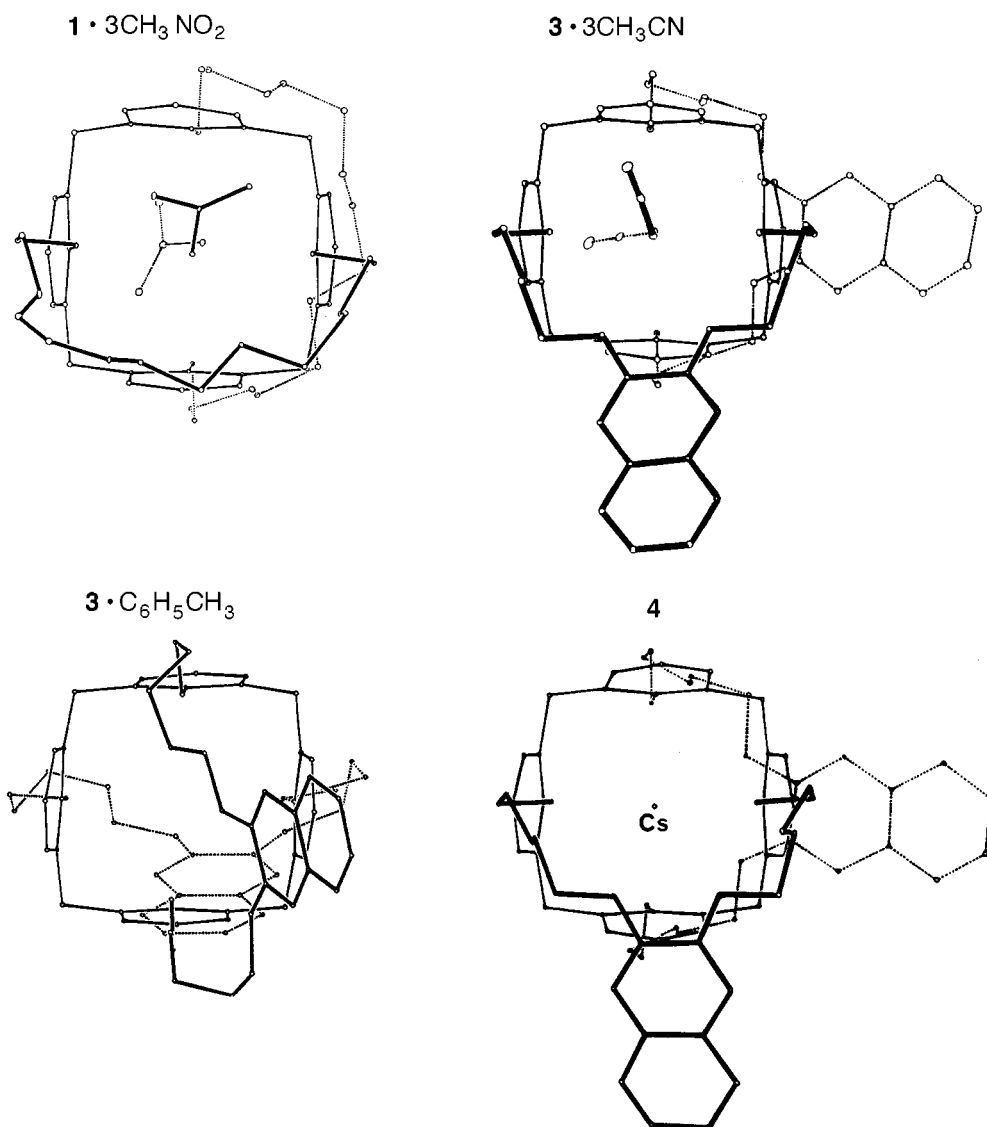


**Fig. 10** Representation of compounds under study, showing the crown conformations. Atoms arbitrarily reduced for clarity. Upper crown and solvent molecule in bold lines, lower ones in dashed lines. Uncomplexed solvent molecules omitted

the zero angle value being a consequence of the presence of the arene ring, allows all the oxygen lone pairs to be directed towards the centre. The essential features of the structure of  $3 \cdot 3\text{CH}_3\text{CN}$  and **4** are nearly identical to those reported for  $2 \cdot 3\text{CH}_3\text{CN}$  and **6** respectively. The presence of the two naphtho groups thus appears not to influence significantly the solvent complexation. The complexed acetonitrile molecules in  $3 \cdot 3\text{CH}_3\text{CN}$  are located with their methyl group near the centre of the crowns [C $\cdots$ O distances between 3.30(2) and 3.62(2): mean 3.46(11) Å]. The six oxygen atoms of each crown are in a plane with a deviation of  $\pm 0.17(1)$  and  $\pm 0.20(1)$  Å respectively, the methyl groups being at 1.06(1) and 1.17(1) Å respectively from these mean planes. This geometry can be compared with those observed in acetonitrile complexes of 18-crown-6 and related compounds:<sup>36</sup> the C $\cdots$ O distances (between 3.3 and 3.7 Å) are comparable to those reported here, however the distances between the methyl group and the oxygen mean plane are longer due to the smaller diameter of the crown ether ring. In these complexes, as in the nitromethane complex cited above,<sup>33</sup> the C–H $\cdots$ O contacts are attributed to very weak acidic hydrogen bonds. An alternative dipole–dipole interaction has also been proposed.<sup>36f</sup> In the acetonitrile complex of a furano-21-crown-7 derivative, comparable in size with the present compound, the C $\cdots$ O distances range from 3.35 to 3.70 Å.<sup>37</sup> A third acetonitrile molecule, badly resolved, is also present in the packing of  $3 \cdot 3\text{CH}_3\text{CN}$ .

In compound **4** the caesium ions lie at the centre of the crown ethers, with Cs–O distances in the range 3.08(1)–3.57(1) [mean 3.30(17)] Å, and at distances of 0.660(1) and 0.735(2) Å from the mean planes defined by the six oxygen atoms of each crown [with deviations of  $\pm 0.34(1)$  and  $\pm 0.37(2)$  Å respectively]. They are also bonded to bidentate nitrate ions with distances in the range 3.10(3)–3.32(3) [mean 3.2(1)] Å and can interact with the  $\pi$  electrons of the two nearer benzene rings, as stated<sup>5–9</sup> [shorter Cs $\cdots$ C distances between 3.38(3) and 3.82(2): mean 3.58(13) Å]. However, the relevance of such  $\pi$  interactions in the caesium selective binding by **1** has recently been questioned.<sup>12</sup>

The most interesting case is that of compound  $3 \cdot \text{C}_6\text{H}_5\text{CH}_3$ , the toluene solvate of **3**. The solvent is not located near the crown ether chains centre and all the intermolecular contacts are greater than 3.5 Å. The resulting crown conformation is very different from that observed in  $3 \cdot 3\text{CH}_3\text{CN}$  and **4**: some *gauche* O–C–O angles become *anti* ones, giving the sequences *ag<sup>-</sup>0ag<sup>+</sup>* and *ag<sup>-</sup>0ag<sup>-</sup>* for the two crowns and some *anti* C–O–C–C angles become *gauche* ones (see Tables 3 and 4). As a result not all the oxygen lone pairs are directed towards the crown centre. The bending of the crown ether moieties is less pronounced than in the other compounds, as can be seen in Fig. 10. The six oxygen atoms of each crown ether moiety cannot be considered as being in a plane (the mean planes are only defined with deviations of  $\pm 0.72$  and  $\pm 0.85$  Å). This case



**Table 3** Selected torsion angles (°) in the crown ether chains of compounds under study

	1·3CH <sub>3</sub> NO <sub>2</sub>		3·3CH <sub>3</sub> CN	3·C <sub>6</sub> H <sub>5</sub> CH <sub>3</sub>	4
C(22)–C(21)–O(1)–C(1)	82(1)	C(38)–C(37)–O(1)–C(1)	–90(1)	82.3(3)	93(2)
C(26)–C(21)–O(1)–C(1)	–99(1)	C(42)–C(37)–O(1)–C(1)	88(1)	–101.4(3)	–87(2)
C(21)–O(1)–C(1)–C(2)	177(1)	C(37)–O(1)–C(1)–C(2)	–176(1)	176.0(2)	174(1)
O(1)–C(1)–C(2)–O(2)	73(1)	O(1)–C(1)–C(2)–O(2)	–74(1)	172.9(2)	68(2)
C(1)–C(2)–O(2)–C(3)	173(1)	C(1)–C(2)–O(2)–C(3)	–169(1)	–163.5(2)	164(1)
C(2)–O(2)–C(3)–C(4)	169(1)	C(2)–O(2)–C(3)–C(4)	179(1)	–80.0(3)	–167(1)
O(2)–C(3)–C(4)–O(3)	–79(1)	O(2)–C(3)–C(4)–O(3)	77(1)	75.8(3)	–76(2)
C(3)–C(4)–O(3)–C(5)	–174(1)	C(3)–C(4)–O(3)–C(5)	172(1)	148.8(2)	174(1)
C(4)–O(3)–C(5)–C(6)	172(1)	C(4)–O(3)–C(5)–C(6)	–171(1)	–155.9(2)	177(1)
O(3)–C(5)–C(6)–O(4)	72(2)	O(3)–C(5)–C(6)–O(4)	–4(2)	–1.5(3)	–2(2)
C(5)–C(6)–O(4)–C(7)	178(1)	C(5)–C(6)–O(4)–C(7)	–178(1)	168.6(2)	–176(1)
C(6)–O(4)–C(7)–C(8)	160(2)	C(6)–O(4)–C(7)–C(8)	–176(1)	–166.0(2)	–173(1)
O(4)–C(7)–C(8)–O(5)	–16(4)	O(4)–C(7)–C(8)–O(5)	–78(1)	176.3(2)	74(2)
C(7)–C(8)–O(5)–C(9)	–131(2)	C(15)–C(16)–O(5)–C(17)	–179(1)	88.4(3)	170(2)
C(8)–O(5)–C(9)–C(10)	–150(2)	C(16)–O(5)–C(17)–C(18)	173(1)	95.9(3)	–163(2)
O(5)–C(9)–C(10)–O(6)	–66(2)	O(5)–C(9)–C(10)–O(6)	74(1)	–67.0(3)	–65(2)
C(9)–C(10)–O(6)–C(36)	177(1)	C(17)–C(18)–O(6)–C(52)	177(1)	–163.6(3)	180(2)
C(10)–O(6)–C(36)–C(35)	84(2)	C(18)–O(6)–C(52)–C(51)	–93(1)	90.7(3)	89(2)
C(10)–O(6)–C(36)–C(37)	–95(1)	C(18)–O(6)–C(52)–C(53)	85(1)	–89.8(2)	–89(2)
C(28)–C(29)–O(7)–C(11)	–92(2)	C(58)–C(59)–O(7)–C(19)	89(1)	–86.2(3)	–85(2)
C(30)–C(29)–O(7)–C(11)	87(2)	C(60)–C(59)–O(7)–C(19)	–91(1)	95.8(3)	93(2)
C(29)–O(7)–C(11)–C(12)	175(1)	C(59)–O(7)–C(19)–C(20)	173(1)	–164.9(3)	169(2)
O(7)–C(11)–C(12)–O(8)	–61(2)	O(7)–C(19)–C(20)–O(8)	73(1)	–62.9(3)	65(2)
C(11)–C(12)–O(8)–C(13)	–171(2)	C(19)–C(20)–O(8)–C(21)	170(1)	97.8(3)	161(2)
C(12)–O(8)–C(13)–C(14)	–176(2)	C(20)–O(8)–C(21)–C(22)	–178(1)	88.8(3)	–163(2)
O(8)–C(13)–C(14)–O(9)	61(2)	O(8)–C(21)–C(22)–O(9)	–75(1)	176.0(2)	–76(2)
C(13)–C(14)–O(9)–C(15)	117(2)	C(21)–C(22)–O(9)–C(23)	–177(1)	–176.9(2)	–173(2)
C(14)–O(9)–C(15)–C(16)	175(2)	C(22)–O(9)–C(23)–C(24)	–178(1)	178.4(2)	175(2)
O(9)–C(15)–C(16)–O(10)	64(2)	O(9)–C(23)–C(24)–O(10)	–1(2)	2.5(4)	2(2)
C(15)–C(16)–O(10)–C(17)	178(1)	C(23)–C(24)–O(10)–C(33)	–174(1)	–166.1(2)	–175(2)
C(16)–O(10)–C(17)–C(18)	–176(1)	C(24)–O(10)–C(33)–C(34)	167(1)	178.6(2)	–180(1)
O(10)–C(17)–C(18)–O(11)	–80(2)	O(10)–C(33)–C(34)–O(11)	77(1)	–62.3(3)	75(2)
C(17)–C(18)–O(11)–C(19)	172(1)	C(33)–C(34)–O(11)–C(35)	–179(1)	96.2(3)	175(2)
C(18)–O(11)–C(19)–C(20)	165(1)	C(34)–O(11)–C(35)–C(36)	–167(1)	88.3(3)	–173(2)
O(11)–C(19)–C(20)–O(12)	74(1)	O(11)–C(35)–C(36)–O(12)	–73(1)	–176.9(2)	–72(2)
C(19)–C(20)–O(12)–C(43)	177(1)	C(35)–C(36)–O(12)–C(45)	–180(1)	–179.9(3)	–171(2)
C(20)–O(12)–C(43)–C(42)	–93(1)	C(36)–O(12)–C(45)–C(44)	89(1)	–88.3(3)	–84(2)
C(20)–O(12)–C(43)–C(44)	90(1)	C(36)–O(12)–C(45)–C(46)	–90(1)	94.8(3)	90(2)

confirms the molecular dynamics calculations, which show the crown ether moieties in those ligands to be highly flexible and only blocked when interacting with ions or solvent molecules.<sup>12</sup>

### Molecular dynamics simulations

The molecular dynamics (MD) simulations *in vacuo* at 300 K have been performed for at least 1 ns on two mononuclear complexes 3·Cs<sup>+</sup> and 3·CsNO<sub>3</sub>, in order to compare X-ray diffraction data with structural averages with a sufficient sampling. The nitrate counter ion appears to have an influence on the cation position, drawing it higher in the crown and slightly out of the mean plane of the six oxygen atoms of the crown [*d*(caesium-plane) = 0.06(32) without nitrate and –0.63(24) Å with nitrate]. The mean *d*(Cs<sup>+</sup>–O) distances, calculated in the case of 3·CsNO<sub>3</sub>, are in reasonable agreement with the X-ray diffraction data, with the exception of atoms O(2) and O(5) (Table 5). These atoms are not neighboured with aryl groups and present a greater affinity with the cation since the corresponding Cs<sup>+</sup>–O distances are smaller. Nevertheless, in spite of a higher point charge on O(2) and O(5) calculated by the MNDO semiempirical method, this feature cannot be evidenced on the Cs<sup>+</sup>–O distances obtained by MD simulations with our force field. We have carried out the MD run on the 3·CsNO<sub>3</sub> complex for a longer time and observed that the cation goes down towards the calixarene cavity after 2 ns. This phenomenon has no impact on the potential energy calculated for minimized structures and seems to be a manifestation of the degrees of freedom left to the cation in the calixcrown.

We have mainly focused on the distribution of O–C–O

dihedral angles in either complexed or uncomplexed crowns (Table 6). On the 1 ns sampling at 300 K, analysed through 996 snapshots, we could compare four uncomplexed and two complexed crowns. The uncomplexed crowns are very mobile (Fig. 11) and the diversity of O–C–O angles collected with respect to the four free crowns considered shows that one 1 ns at 300 K is not sufficient to obtain an accurate sampling. The simulation on 3·CsNO<sub>3</sub> was then carried out up to 5 ns with a control stop every 800 ps. In the 5 ns sampling the number of conformations collected is 42, the main ones being the same as in the corresponding 1 ns sampling, which suggests that a longer time is still needed at 300 K to obtain a statistical distribution independent of the starting structure. Conformations with one or two *anti* angles represent 83% of the sampling. This preference for the presence of *anti* angles in the free crown is illustrated by the crystal structure of 3 crystallized from toluene, a non-polar solvent which interacts poorly with the crown (see above).

The introduction of a guest in the crown, here a caesium cation, reduces considerably the crown mobility and *anti* dihedral angles are no longer sampled. With an additional nitrate counter ion we observe only O(2)–C–O(3) and O(4)–C–O(5) *g*<sup>+</sup>↔*g*<sup>–</sup> transitions, giving the experimental *g*<sup>+</sup>*g*<sup>–</sup>0*g*<sup>+</sup>*g*<sup>–</sup> as the main conformation, although its percentage varies with the amount of sampling to become stabilized above 3.4 ns. Here also we wonder about the accuracy of the sampling, as the rigidity of the molecular system renders this more difficult at 300 K.

A control run of 1 ns at 500 K was then performed on 3·CsNO<sub>3</sub>. For the free crown all the possible conformations (45) were sampled, 80% of which having one or two *anti* angles and 16% having only *gauche* ones. For the complexed crown 10 conformations involving only *gauche* angles were sampled,

**Table 4** Crown ether conformations in compounds **1**, **2**, **3** and **5**

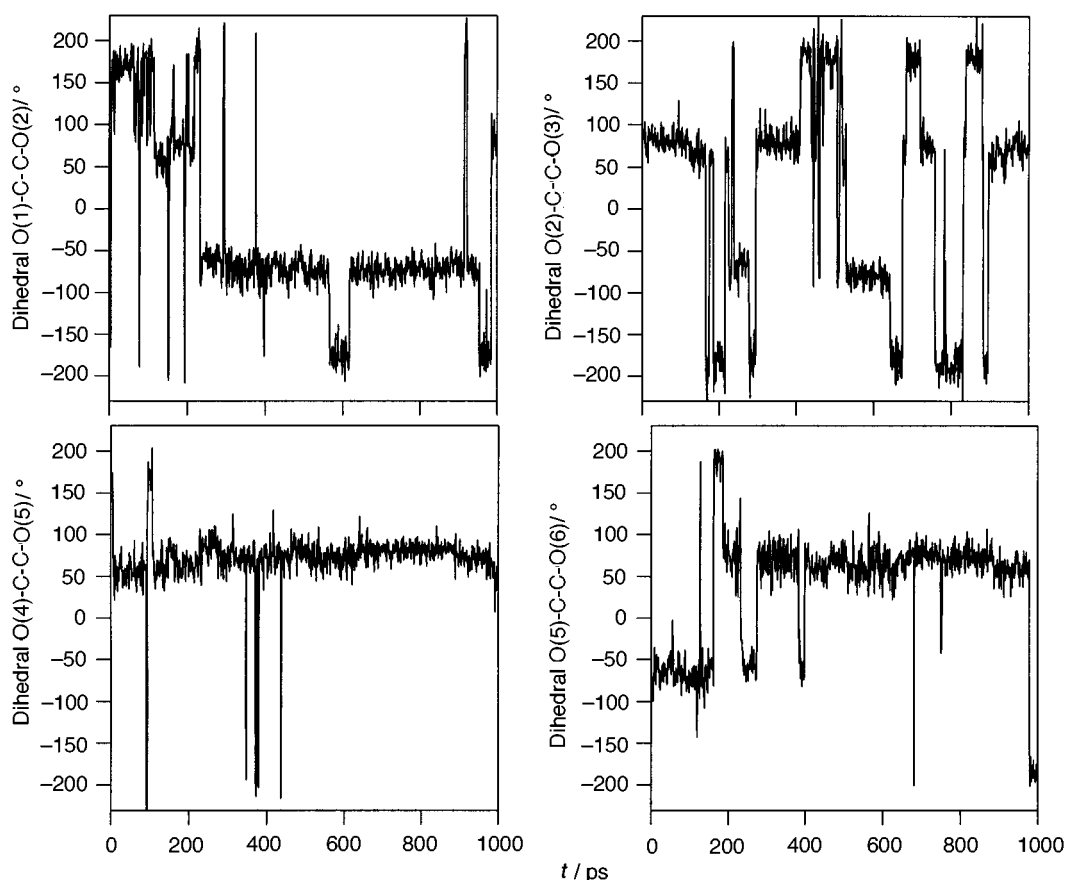
	Conformation <sup>a</sup>	Number of C–O–C		Compounds
		<i>anti</i> → <i>gauche</i> transformations <sup>b</sup>	Number of occurrences	
<b>5</b>	$g^+g^-g^+g^-$	1	1	$Cs^+ \cdot ^-OC_6H_2(NO_3)_3-2,4,6 \cdot 5 \cdot 0.5CHCl_3$ <sup>32</sup>
	$g^-g^+g^-g^+$	1	1	$Cs^+ \cdot ^-OC_6H_2(NO_3)_3-2,4,6 \cdot 5 \cdot 0.5CHCl_3$ <sup>32</sup>
<b>1</b>	$g^+g^-g^+g^-$	0	6	$1 \cdot 4CH_3CN$ , <sup>6</sup> $1 \cdot 3CH_3CN$ , <sup>8</sup> $Cs^+ \cdot NO_3^- \cdot 1 \cdot 2CH_3CN$ , <sup>6</sup> $2Cs^+ \cdot 2NO_3^- \cdot 1 \cdot 2CH_3CN$ , <sup>6</sup> $2Cs^+ \cdot 2NO_3^- \cdot 1$ , <sup>6</sup> $K^+ \cdot NO_3^- \cdot 1 \cdot 2CH_3CN$ <sup>9</sup>
	$g^+g^-g^+g^-$	0 or 1	4	$1 \cdot 3CH_3NO_2$ , $2Cs^+ \cdot 2NCS^- \cdot 1$ , <sup>5</sup> $2Cs^+ \cdot 2I^- \cdot 1 \cdot 2CH_3CN$ , <sup>7</sup> $2Na^+ \cdot 2NO_3^- \cdot 1 \cdot 2H_2O \cdot CH_3CN$ <sup>9</sup>
	$g^+g^+g^-g^-$	2	2	$2Cs^+ \cdot 2NO_3^- \cdot 1$ , <sup>6</sup> $2Cs^+ \cdot 2NCS^- \cdot 1$ <sup>5</sup>
	$g^+g^-g^+g^-$	1	1	$2Na^+ \cdot 2NO_3^- \cdot 1 \cdot 2H_2O \cdot CH_3CN$ <sup>9</sup>
	$g^+g^-0g^+g^-$	0	1	$1 \cdot 3CH_3CN$ <sup>8</sup>
	$g^+g^-g^+(\approx 16^\circ)g^-$	0	1	$1 \cdot 3CH_3NO_2$
	$g^+g^-0g^+g^-$	0	3	$2 \cdot 3CH_3CN$ , <sup>8</sup> $2 \cdot 3CH_3NO_2$ , <sup>35</sup> <b>6</b> <sup>5</sup>
<b>2</b>	$g^+g^-0g^+g^-$	0	2	<b>3</b> · $3CH_3CN$ , <b>4</b>
	$ag^+0ag^-$	3	1	<b>3</b> · $C_6H_5CH_3$
<b>3</b>	$ag^-0ag^-$	4	1	<b>3</b> · $C_6H_5CH_3$

<sup>a</sup> Sequence of O–C–O torsion angles. <sup>b</sup> The C–O–C angles involving calixarene carbon atoms are not taken into account.

**Table 5** Average structural data in **3**· $Cs^+$  and **3**· $CsNO_3$  complexed crowns during the molecular dynamics run *in vacuo* at 300 K

Compound	$d(Cs-O)/\text{\AA}$						$\langle d(Cs-O) \rangle / \text{\AA}$
	O(1)	O(2)	O(3)	O(4)	O(5)	O(6)	
<b>3</b> · $Cs^+$ (1 ns <sup>b</sup> )	3.04(13)	3.39(25)	3.35(23)	3.34(23)	3.40(26)	3.04(13)	3.26(16)
<b>3</b> · $CsNO_3$ (1 ns)	3.38(24)	3.36(22)	3.49(29)	3.52(33)	3.32(21)	3.47(26)	3.42(8)
	(3.4 ns)	3.30(25)	3.37(24)	3.65(37)	3.67(39)	3.34(24)	3.32(27)
<b>3</b> · $2CsNO_3$ (XRD) (crown 1)	3.22(1)	3.08(1)	3.51(1)	3.57(1)	3.13(1)	3.22(1)	3.30(17)
	(crown 2)	3.37(1)	3.17(2)	3.51(2)	3.47(2)	3.16(1)	

<sup>a</sup> Average over the individual  $d(Cs-O)$  values. <sup>b</sup> Averages were calculated on 996 (1) or 3396 snapshots (3.4 ns).

**Fig. 11** Time evolution of dihedral O–C–O angles in **3**· $CsNO_3$  uncomplexed crown during a 1 ns molecular dynamics run *in vacuo* at 300 K

**Table 6** Conformation sampling of O–C–C–O dihedral angles during the molecular dynamics runs *in vacuo*

	<b>3</b>	<b>3·Cs<sup>+</sup></b>	<b>3·CsNO<sub>3</sub></b>	<b>3·CsNO<sub>3</sub></b>	<b>3·CsNO<sub>3</sub></b>	<b>3·CsNO<sub>3</sub></b>
Number of snapshots	993 (1 ns)	996 (1 ns)	996 (1 ns)	3396 (3.4 ns)	4996 (5 ns)	996 (1 ns)
<i>T/K</i>	300	300	300	300	300	500
Crown 1	Uncomplexed	Complexed	Complexed	Complexed	Complexed	Complexed
Number of conformations	17	10	3	4	4	12
Main conformations	$g^+a0g^+g^-$ 205 $g^+a0g^-g^+$ 194 $g^+g^+0g^-g^+$ 147 $g^+g^+0g^-a$ 84 $g^+a0g^-a$ 80	$g^+g^+0g^-g^-$ 450 $g^-g^+0g^-g^+$ 157 $g^-g^+0g^-g^-$ 130	$g^+g^-0g^+g^-$ 816 (82%) $g^+g^-0g^-g^-$ 152 (15%) $g^+g^+0g^+g^-$ 28 (3%)	$g^+g^-0g^+g^-$ 2219 (65%) $g^+g^-0g^-g^-$ 736 (22%) $g^+g^+0g^+g^-$ 439 (13%) $g^+g^+0g^-g^-$ 2	$g^+g^-0g^+g^-$ 3233 (65%) $g^+g^-0g^-g^-$ 1020 (20%) $g^+g^+0g^+g^-$ 735 (15%) $g^+g^+0g^-g^-$ 8	$g^+g^-0g^+g^-$ 487 (49%) $g^+g^-0g^-g^-$ 155 (16%) $g^+g^+0g^+g^-$ 159 (16%)
Crown 2	Uncomplexed	Uncomplexed	Uncomplexed	Uncomplexed	Uncomplexed	Uncomplexed
Number of conformations	21	14	11	33	42	45
Main conformations	$g^+g^+0ag^-$ 298 $g^+g^+0g^+g^-$ 273 $g^+g^+0g^+a$ 85 $g^+g^+0g^-g^-$ 78	$g^-g^+0g^+g^-$ 461 $g^-g^+0ag^-$ 222 $ag^+0ag^-$ 97	$g^+g^+0g^+a$ 459 $g^+g^+0g^+g^-$ 267 $g^+a0g^+a$ 98	$g^+g^+0g^+a$ 801 $g^+g^+0g^+g^-$ 333 $ag^+0g^-a$ 325 $g^+a0g^+a$ 89	$g^+g^+0g^+a$ 806 (16%) $g^+g^+0g^+g^-$ 448 (9%) $ag^+0g^-a$ 422 (8%) $g^+a0g^+a$ 416 (8%)	$g^-a0g^+a$ 93 (9%) $g^-a0g^-a$ 60 (6%) $g^+g^-0ag^-$ 54 (5%) $g^-g^+0g^+a$ 49 (5%)

here also the main ones are  $g^+g^-0g^+g^-$  (49%),  $g^+g^-0g^-g^-$  (16%) and  $g^+g^+0g^+g^-$  (16%). Only three snapshots over 996 involved one *anti* angle. These results at 500 K show that the 5 ns at 300 K have previously given a quite good representative sampling of the crown conformations. Our molecular dynamics simulations *in vacuo* point out the absence of an intrinsic preorganization of the free crowns which can adopt most of the possible conformations involving up to two non-adjacent *anti* O–C–C–O dihedral angles. Upon complexation, *anti* dihedral angles disappear but the crown retains some conformational freedom which diminishes with the presence of a bulky species in front of the crown (in our simulation, the nitrate counter ion).

## Conclusion

The crystal structures reported in this work, as well as those determined earlier, show that calix[4]arene bis(18-crown-6) and its benzo and naphtho derivatives can form complexes with solvent molecules such as acetonitrile and nitromethane, able to form weak hydrogen bonds with ether oxygen atoms. The resulting crown conformation, in the case of compound **3**, is different from that of the empty crown. In all cases the conformation in the solvent complexes is the same, or only slightly different, from that in the caesium complexes. The molecular dynamics calculations were performed *in vacuo* and do not enable one to elucidate the solvent effect in the complexation. However, the preorganization (as defined by Cram<sup>38</sup>) of ligands, and particularly macrocycles, by solvent molecules, leading to a minimization of conformational changes upon complexation of particular species, has been the subject of numerous investigations. In the present field some computational studies have been performed on solvent-induced conformational changes in crown ether systems<sup>39–41</sup> and calixarene derivatives.<sup>42,43</sup> Some experimental work has also been reported in the case of *p*-*tert*-butylcalix[4]arene tetraacetate:<sup>44</sup> in this case the solvent (in the hydrophobic cavity) is thought to exert an allosteric effect which facilitates complexation of alkali-metal ions in the hydrophilic site. In our case a higher caesium over sodium selectivity has been experimentally observed for **3** and **2** than for **1**: this has been attributed, not to a more efficient caesium complexation, but to a lower sodium affinity.<sup>29</sup> The preorganization for caesium complexation may be a less important trend in this case than the rigidity of the crown induced by the arene substituents which prevents a convenient geometry for the sodium ion complexation from being attained.

## References

- Z. Asfari, C. Bressot, J. Vicens, C. Hill, J. F. Dozol, H. Rouquette, S. Eymard, V. Lamare and B. Tournois, *Anal. Chem.*, 1995, **67**, 3133.
- Z. Asfari, S. Wenger and J. Vicens, *J. Incl. Phenom.*, 1994, **19**, 137; C. Hill, J. F. Dozol, V. Lamare, H. Rouquette, S. Eymard, B. Tournois, J. Vicens, Z. Asfari, C. Bressot, R. Ungaro and A. Casnati, *J. Incl. Phenom.*, 1994, **19**, 399.
- Z. Asfari, M. Nierlich, P. Thuéry, V. Lamare, J. F. Dozol, M. Leroy and J. Vicens, *An. Quím. Int. Ed.*, 1996, **92**, 260.
- T. J. Haverlock, P. V. Bonnesen, R. A. Sachleben and B. A. Moyer, *Radiochim. Acta*, 1997, **76**, 103.
- P. Thuéry, M. Nierlich, C. Bressot, V. Lamare, J. F. Dozol, Z. Asfari and J. Vicens, *J. Incl. Phenom.*, 1996, **23**, 305.
- Z. Asfari, C. Naumann, J. Vicens, M. Nierlich, P. Thuéry, C. Bressot, V. Lamare and J. F. Dozol, *New J. Chem.*, 1996, **20**, 1183.
- P. Thuéry, M. Nierlich, V. Lamare, J. F. Dozol, Z. Asfari and J. Vicens, *Acta Crystallogr., Sect. C*, 1996, **52**, 2729.
- P. Thuéry, M. Nierlich, Z. Asfari and J. Vicens, *J. Incl. Phenom.*, 1997, **27**, 169.
- P. Thuéry, M. Nierlich, V. Lamare, J. F. Dozol, Z. Asfari and J. Vicens, *Supramol. Chem.*, in the press.
- V. Lamare, C. Bressot, J. F. Dozol, J. Vicens, Z. Asfari, R. Ungaro and A. Casnati, *Sep. Sci. Technol.*, 1997, **32**, 175.
- G. Wipff and M. Lauterbach, *Supramol. Chem.*, 1995, **6**, 187.
- A. Varnek and G. Wipff, *J. Mol. Struct. (Theochem)*, 1996, **363**, 67.
- G. M. Sheldrick, SHELXS 86, Program for the Solution of Crystal Structures, University of Göttingen, 1985.
- International Tables for X-Ray Crystallography*, Kynoch Press, Birmingham, 1974, vol. 4; present distributor: Academic Publishers, Dordrecht.
- MOLEN: An Interactive Structure Solution Procedure, Enraf-Nonius, Delft, 1990.
- K. Harms, XCAD 4, University of Marburg, 1995.
- SHELXTL, Version 5/IRIX, Siemens Analytical X-ray Instruments, Madison, WI, 1990.
- A. L. Spek, *Acta Crystallogr., Sect. A*, 1990, **46**, C-34.
- C. K. Johnson, ORTEP II, Report ORNL-5138, Oak Ridge National Laboratory, Oak Ridge, TN, 1976.
- D. A. Pearlman, D. A. Case, J. A. Caldwell, W. S. Ross, T. E. Cheatham III, D. M. Ferguson, G. L. Seibel, U. C. Singh, P. Weiner and P. A. Kollman, AMBER 4.1, University of California, San Francisco, 1995.
- S. J. Weiner, P. A. Kollman, D. T. Nguyen and D. A. Case, *J. Comput. Chem.*, 1986, **7**, 230.
- SYBYL 6.1, Molecular Modeling Software, TRIPOS Inc., 1994.
- T. J. Marrone, D. S. Hartsough and K. M. Merz, *J. Phys. Chem.*, 1994, **98**, 1341.
- J. Åqvist, *J. Phys. Chem.*, 1990, **94**, 8021.
- P. Guilbaud and G. Wipff, *J. Phys. Chem.*, 1993, **97**, 5685.
- E. Engler and G. Wipff, MDS and MD/DRAW 1.0, Laboratoire de Modélisation et de Simulations Moléculaires (MSM), Université Louis Pasteur, Strasbourg.
- A. Ikeda, H. Tsuzuki and S. Shinkai, *Tetrahedron Lett.*, 1994, 8417; A. Ikeda and S. Shinkai, *J. Am. Chem. Soc.*, 1994, **116**, 3102.
- P. D. Beer, M. G. B. Drew, P. A. Gale, P. B. Leeson and M. I. Ogden, *J. Chem. Soc., Dalton Trans.*, 1994, 3479.
- F. Arnaud-Neu, Z. Asfari, B. Souley and J. Vicens, *New J. Chem.*, 1996, **20**, 453.
- T. M. Fyles and R. D. Gandour, *J. Incl. Phenom.*, 1992, **12**, 313.
- Handbook of Chemistry and Physics*, ed. D. R. Lide, CRC Press, Boca Raton, FL, 72nd edn., 1992, pp. 15–43.
- R. Ungaro, A. Casnati, F. Uguzzoli, A. Pochini, J. F. Dozol, C. Hill and H. Rouquette, *Angew. Chem., Int. Ed. Engl.*, 1994, **33**, 1506.
- J. A. A. de Boer, D. N. Reinhoudt, S. Harkema, G. J. van Hummel and F. de Jong, *J. Am. Chem. Soc.*, 1982, **104**, 4073.
- J. H. Burns, J. C. Bryan, M. C. Davis and R. A. Sachleben, *J. Incl. Phenom.*, 1996, **26**, 197.
- P. Thuéry, M. Nierlich, Z. Asfari and J. Vicens, unpublished work.
- See, for example: (a) B. L. Allwood, S. E. Fuller, P. C. Y. K. Ning, A. M. Z. Slawin, J. F. Stoddart and D. J. Williams, *J. Chem. Soc., Chem. Commun.*, 1984, 1356; (b) R. D. Rogers, P. D. Richards and E. J. Voss, *J. Incl. Phenom.*, 1988, **6**, 65; (c) R. L. Garrell, J. C. Smyth, F. R. Fronczek and R. D. Gandour, *J. Incl. Phenom.*, 1988, **6**, 73; (d) R. D. Rogers, *J. Incl. Phenom.*, 1988, **6**, 629; (e) F. Weller, H. Borgholte, H. Stenger, S. Vogler and K. Dehnicke, *Z. Naturforsch., Teil B*, 1989, **44**, 1524; (f) K. Panneerselvam, K. K. Chacko, E. Weber and H. J. Köhler, *J. Incl. Phenom.*, 1990, **9**, 337; (g) M. R. Caira and R. Mohamed, *Acta Crystallogr., Sect. B*, 1993, **49**, 760; (h) F. Vögtle, W. M. Müller and W. H. Watson, *Top. Curr. Chem.*, 1984, **125**, 131.
- J. H. Burns, personal communication.
- D. J. Cram, *Angew. Chem., Int. Ed. Engl.*, 1988, **27**, 1009.
- G. Ranghino, S. Romano, J. M. Lehn and G. Wipff, *J. Am. Chem. Soc.*, 1985, **107**, 7873.
- L. Troxler and G. Wipff, *J. Am. Chem. Soc.*, 1994, **116**, 1468.
- G. Wipff and L. Troxler, in *Computational Approaches in Supramolecular Chemistry*, ed. G. Wipff, Kluwer, Dordrecht, 1994, p. 319.
- A. Varnek and G. Wipff, *J. Phys. Chem.*, 1993, **97**, 10 840.
- P. Guilbaud, A. Varnek and G. Wipff, *J. Am. Chem. Soc.*, 1993, **115**, 8298.
- A. F. Danil de Namor, N. Apaza de Sueros, M. A. McKervey, G. Barrett, F. Arnaud Neu and M. J. Schwing-Weill, *J. Chem. Soc., Chem. Commun.*, 1991, 1546.

Received 28th July 1997; Paper 7/05453J